nature catalysis

Article

https://doi.org/10.1038/s41929-025-01340-7

Organocatalytic regio- and stereoselective cyclopropanation of olefins

Received: 27 August 2024

Accepted: 9 April 2025

Published online: 16 May 2025

Check for updates

Chendan Zhu[1,2], Sayantani Das[1,2], Avishek Guin[1], Chandra Kanta De[1] & Benjamin List[1]

As reactive intermediates and substructures of natural products and bioactive molecules, the smallest cyclic alkanes—cyclopropanes—are an attractive class of molecules for chemists. Arguably, the most general approach to their chemical synthesis involves the addition of metal carbenes to olefins. Whereas catalytic asymmetric cyclopropanations of electronically unbiased olefins with carbenoids have been reported using chiral metal complexes and engineered metalloenzymes, we now report a complementary, metal-free and highly enantioselective cyclopropanation of olefins with diazoalkanes, applying asymmetric counteranion-directed photoredox organocatalysis. We identify an ion pair featuring a thioxanthylium photoredox cation and a chiral imidodiphosphorimidate counteranion that catalyses highly enantioselective cyclopropanations of styrenes and aliphatic dienes with diazo compounds. Mechanistic investigations reveal a wavelength dependence of the enantioselectivity and suggest that the main catalytic pathway proceeds via olefin-derived radical cation intermediates. This metal-free, highly enantioselective organocatalytic approach complements previously reported methods for alkene manipulations.

The synthesis of cyclopropanes[1–4] via metal-catalysed carbene transfer from diazo compounds to olefins[5–8] is among the best developed and most general cyclopropanations available. Enantioselective versions are documented, both with chiral metal complexes as catalysts and with engineered metalloenzymes. High effectiveness and stereocontrol have been accomplished with catalysts based on copper[9], rhodium[10] and ruthenium[11]. In particular, excellent levels of enantioselectivity have been achieved with copper(I) bisoxazoline complexes[12] and with dinuclear rhodium(II) complexes, featuring chiral bidentate carboxylate, amidate or phosphate ligands[13–15]. A unique nickel carbene mediated cyclopropanation has also been reported[16].

Biocatalytic, new-to-nature versions of this reaction were reported by Arnold et al. in 2013[17], using an engineered cytochrome P450 enzyme that catalyses highly diastereo- and enantioselective cyclopropanations of styrenes with diazoesters. The Hartwig group developed iridium-modified myoglobins that catalyse the cyclopropanation of unactivated olefins[18], and the Keasling group[19] described a variant in which both the diazoester and the styrene were produced intracellularly. While the biocatalytic and the transition metal catalysed approaches are conceptually different, they share the initial formation of electrophilic metal carbenoids, which then engage in the actual olefin cyclopropanation (Fig. 1a). Despite these advancements, regioselectivity for substrates with multiple olefins remains a particularly challenging problem[20–23]. We became intrigued by the idea of designing a complementary organocatalytic approach that would not necessitate the involvement of metal carbenoids and could solve the regioselectivity problem. Organocatalytic cyclopropanations of olefins activated by an electron-withdrawing group have previously been reported[24–26] but those of electronically unbiased olefins are unknown. Since organocatalytic activation modes for diazo alkanes or olefins, other than protonation by Brønsted acids, which appeared not to be suitable for the desired process, are not available, such a design immediately led

[1]Max-Planck-Institut für Kohlenforschung, Mülheim an der Ruhr, Germany. [2]These authors contributed equally: Chendan Zhu, Sayantani Das.
e-mail: de@kofo.mpg.de; list@kofo.mpg.de

https://doi.org/10.1038/s41929-025-01340-7

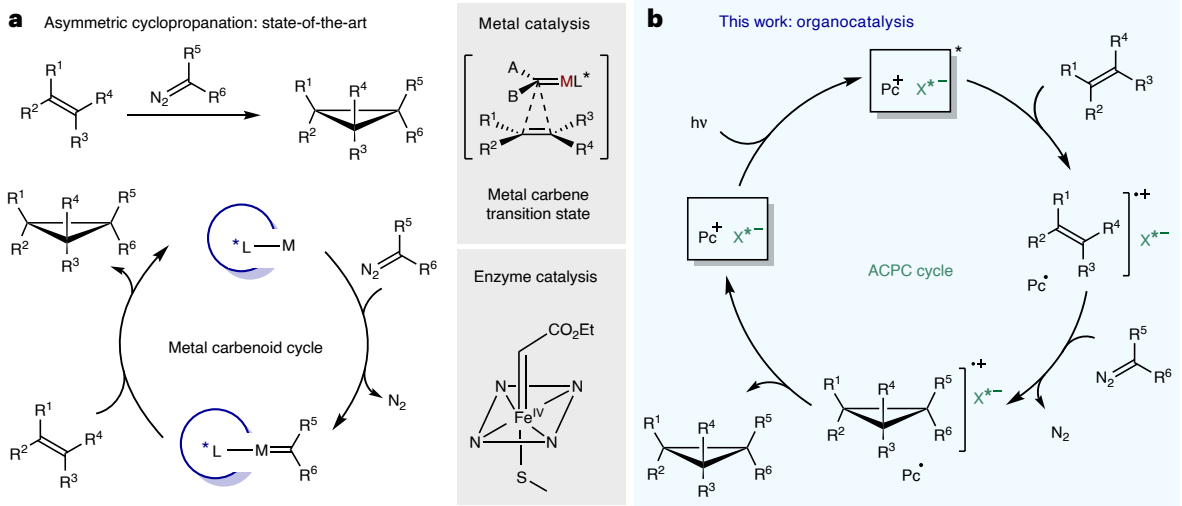

Fig. 1 | Asymmetric cyclopropanation between olefin and diazo compound. a, State-of-the-art approaches to cyclopropanation of olefin with diazo compounds using metal catalysts, enzyme catalysts and the catalytic cycle. **b**, Our design, featuring catalytic asymmetric insertion of a diazo compound to an in situ-generated radical cation intermediate. L, ligand; M, metal.

to the challenge of how to organocatalytically activate simple olefins and/or diazo esters. We hypothesized that the abstraction of a single electron—arguably the most general strategy for activating any molecule—could be suitable here. Accordingly, we envisioned a catalytic cycle in which the olefin is activated as a radical cation upon single electron transfer to a photoexcited cationic organocatalyst associated with an enantiopure counteranion. The resulting highly reactive open-shell radical cation forms an ion pair with the enantiopure counteranion and is expected to undergo enantioselective carbon–carbon bond formation with the diazoalkane, accompanied by the loss of N_2 to furnish a cyclopropane radical cation[27–29]. A final single electron transfer from the catalyst radical to this intermediate should then regenerate the cationic photocatalyst and deliver the desired cyclopropane product (Fig. 1b). This design is supported by a recently established radical cation-based photoredox catalytic cyclopropanation[27] and by our own work on utilizing enantiopure counteranions in photoredox catalytic cycloadditions via olefin-derived radical cations[30]. The envisioned challenges associated with our concept are controlling the facial selectivity of a highly reactive open-shell radical cation intermediate and preventing the direct activation of diazoalkane to a free carbene via photolysis or energy transfer from the excited state photocatalyst, which could lead to racemic products[31–33].

Herein, we report an organocatalytic regio- and stereoselective cyclopropanation of olefins, facilitated by asymmetric counteranion-directed photoredox catalysis (ACPC).

Results

Reaction development

To initiate our investigation, we studied the cyclopropanation reaction of *trans*-anethole (**1a**) and diazoester **2a** in a (1:1 v/v) solvent mixture of dichloromethane (CH_2Cl_2) and pentane at −100 °C under irradiation by 6 W of green light. We began by exchanging the counteranion of the synthesized thioxanthylium triflate[34] organophotoredox catalyst with different confined imidodiphosphorimidate (IDPi)[35] anions (Fig. 2). Encouraged by our previous studies on IDPi-catalyzed transformations, we initially selected from our assortment of privileged IDPi anions. An IDPi catalyst possessing a para-*tert*-butyl group as 3,3′ substituent and a trifyl core (IDPi-**A**) delivered the corresponding cyclopropanated product with moderate yield, good enantioselectivity (80:20 er) and poor diastereoselectivity. An analogous meta-biphenyl IDPi (IDPi-**B**) gave improved yield (90%) and enantioselectivity (90:10 er). Using catalyst **4C** where the 3,3′ substituents of the IDPi catalyst feature a combination of *meta*- and *para*-substitution, led to a further enhancement of the enantioselectivity (95:5 er) with a dr of roughly 3:1. Having identified an optimal catalyst towards enantioselectivity, we were keen to further improve the diastereoselectivity. In this regard, *meta*-,*para*-substituted catalysts were extensively evaluated (Supplementary Table 1), and among them, spirocyclic fluorenyl substitution on the 3,3′-positions of the BINOL was found to be suitable towards this aim (**4D**–**F**). To our delight, the modified spirocyclopentyl fluorenyl substitution on the 3,3′-positions of the BINOL (IDPi-**E**) delivered the product not only with excellent yield and enantioselectivity but also with excellent diastereoselectivity of >20:1. Finally, fine-tuning of the inner core sulfonamide from trifluoromethyl (IDPi-**E**) to *n*-perfluoroethyl (IDPi-**F**) enhanced the enantiomeric ratio from 97:3 to 99:1, maintaining the excellent yield and diastereoselectivity. Remarkably, even at −100 °C, catalyst **4F** rapidly furnished product **3a** in a short reaction time. Lowering the catalyst loading from 2.5 to 0.5 mol% still gave full conversion with high yield even though a slight reduction of enantioselectivity (96:4 er) was observed.

Substrate scope

Next, a broad range of olefins with different double bond location and substituents at different ring positions were evaluated (Fig. 3) in the reaction with diazoester derivatives, and the cyclopropane products were obtained with good to excellent yields and enantioselectivities. Moreover, most of these products were obtained with excellent diastereoselectivities. 3-Ethyl anethole was found to be a suitable reaction partner and furnished product **3b** with excellent enantioselectivity. Interestingly, 3,3-dimethyl anethole also delivered the desired product (**3c**) with excellent enantioselectivity, albeit with low diastereoselectivity. An olefin bearing an *tert*-butyldimethylsilyloxy (OTBS) substituent was also tolerated, providing product **3d** with an er of 97:3 in 86% yield. Similarly, olefins featuring electron-withdrawing substituents and a heterocyclic ring furnished products **3e** and **3f** in excellent enantioselectivities. It is worth mentioning that other electron-rich heterocyclic olefins successfully engaged in our cyclopropanation and furnished products **3g** and **3h** with good to excellent level of enantioselectivity. Next, we focused on using electron neutral styrene derivatives as potential olefins for cyclopropanation. As their redox potential (>1.8 V) is higher than that of the used thioxanthylium photocatalyst (1.76 V), a photocatalyst featuring a higher redox potential was

https://doi.org/10.1038/s41929-025-01340-7

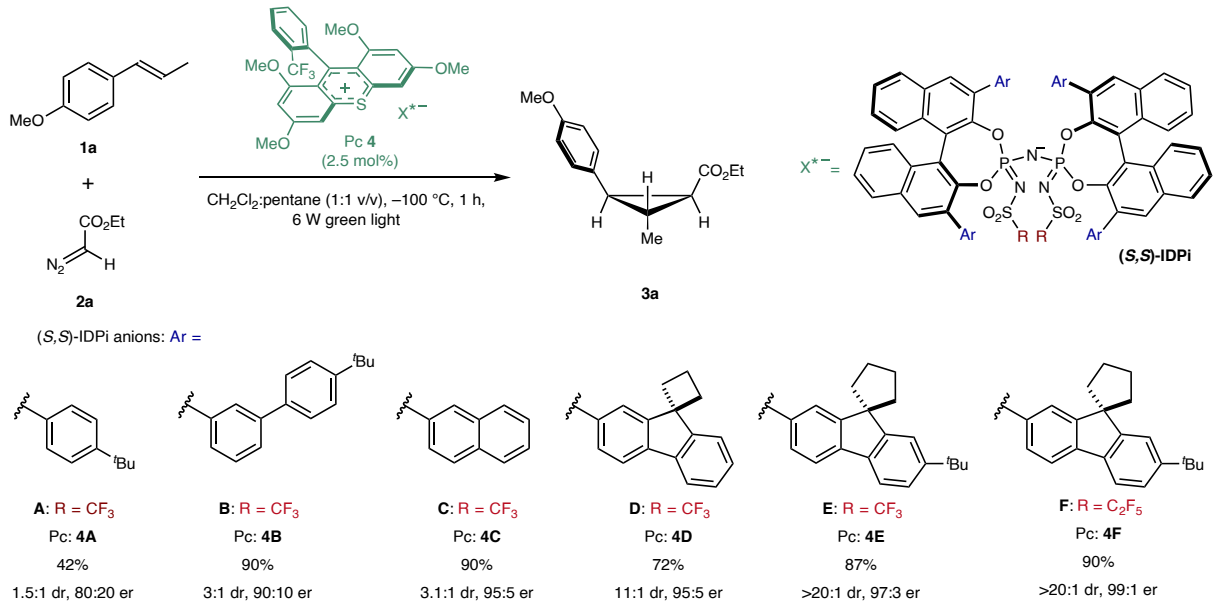

Fig. 2 | Reaction development. Optimization of the catalytic reaction for the evaluation of IDPi anions was carried out, and the yield was determined by ^{1}H NMR using an internal standard.

required. Gratifyingly, acridinium photocatalyst **5** (2.04 V), under red light irradiation, delivered products **3i** and **3j** with excellent enantioselectivity. Internal olefins gave products **3k** and **3l** in good yields and excellent enantioselectivity. We explored different diazoesters and found that all of the different diazoesters gave the desired products (**3m** and **3n**) with an excellent level of enantioselectivity. Additionally, a disubstituted diazoester was found to be a suitable partner for our cyclopropanation reaction and yielded the desired product **3o** in good enantioselectivity and moderate diastereoselectivity. We also investigated a diazoalkanes featuring an N-H amide-, aromatic or aliphatic keto functionality, and all furnished the desired products (**3p**–**r**) with *trans*-anethole in moderate to good level of enantioselectivity. Finally, even trimethylsilyl-diazomethane reacted to product **3s** with promising results.

Having successfully developed an organocatalytic cyclopropanation of olefins, we wondered whether our confined catalyst design may enable selectivity also with substrates bearing multiple olefins. For example, 2,5-dimethylhexa-2,4-diene (**1t**) is a symmetrical diene that has previously been used in the synthesis of chrysanthemic acid, a natural product also found in a variety of insecticides. In this case, the chemoselectivity issue towards obtaining the corresponding monocyclopropane has previously only been overcome by using a several fold excess of the diene[23]. Remarkably, using our organocatalyst system, chrysanthemic acid derivative **3t** could be obtained selectively in good yield and good enantioselectivity for both diastereomers without requiring an excess of diene. Subsequently, a simple hydrolysis of ester **3t** gave chrysanthemic acid (**3u**), preserving the enantioselectivity (Fig. 3b). We further explored the reactions of unsymmetrical conjugated dienes and trienes, delivering the desired products in good yield and enantioselectivities.

It is noteworthy that an unsymmetrical conjugated diene delivered product **3v** with remarkable regioselectivity (>20:1 rr) and diastereoselectivity (>20:1 dr). A diene substrate bearing an additional pendant olefin functionality (**1w**) was also found to be suitable for our cyclopropanation. Even the reaction with conjugated and unsymmetrical triene **1x**, posing a formidable regioselectivity challenge, selectively delivered product **3x** (Fig. 3c). On the other hand, we also recognized the limitations of our reaction (Supplementary Fig. 2). Olefins bearing electron-withdrawing groups yielded the desired product in low amounts but with high enantioselectivity. Unfortunately, substrates containing amino-substituted aryl groups, indole-derived olefins, enol ethers and enamines remained unreactive under our reaction conditions. Additional diazo compounds were tested, furnishing the desired product in moderate to good yields with satisfactory enantioselectivity. However, we observed that acceptor–acceptor diazoalkanes did not undergo the transformation. Additionally, enantioenriched product **3a** was derivatized to carboxylic acid product **6** without any loss of selectivities. Furthermore, a sequential reduction of the ethyl ester of **3a** to the corresponding alcohol, followed by Steglich esterification gave ferrocene ester **7**, the absolute configuration of which could be determined by single crystal X-ray diffraction.

Mechanistic investigations

During our reaction development, lowering the catalyst loading from 2.5 to 0.5 mol% still gave full conversion with a high yield. However, a slight reduction of enantioselectivity was observed (Fig. 4a). Furthermore, the amount of diazoester was evaluated. Surprisingly, increasing the amount of the diazoester also led to a reduction of enantioselectivity (Fig. 4b). These two results hinted at a non-enantioselective, photochemical background pathway[31–33]. Since such a background reactivity may require a different wavelength, we were intrigued to explore light of different wavelengths. Indeed, a red shift was associated with a notable increase of enantioselectivity (Fig. 4c). To gain further insight into this phenomenon, we irradiated our model substrate **1a** and diazoester **2a** with blue or yellow light separately. Remarkably, irradiation with yellow light led to higher enantioselectivity, from 80% ee with blue light to 97% ee with yellow light. Similarly, when olefin substrates **1k** and **1l** were excited with yellow instead of blue light under similar conditions, an increase in enantioselectivity was observed. For example, for product **3l**, the enantiomeric excess increased from 41.8% with blue light to 95.4% with yellow light (Fig. 4d).

To shed light on this unusual observation, we conducted absorption spectroscopy of diazoester and photocatalyst, where diazoester **2a** has a maximum wavelenth of absorption (λ_{max}) at 397 nm (Fig. 5a) and photocatalyst **4F** has a λ_{max} at 472 nm (Fig. 5b). Since the absorption band of photocatalyst **4F** is very broad, the opportunity arose to excite the photocatalyst at different wavelengths and study the corresponding emission spectra. Photocatalyst **4F** was excited at 472 nm (λ_{max})

https://doi.org/10.1038/s41929-025-01340-7

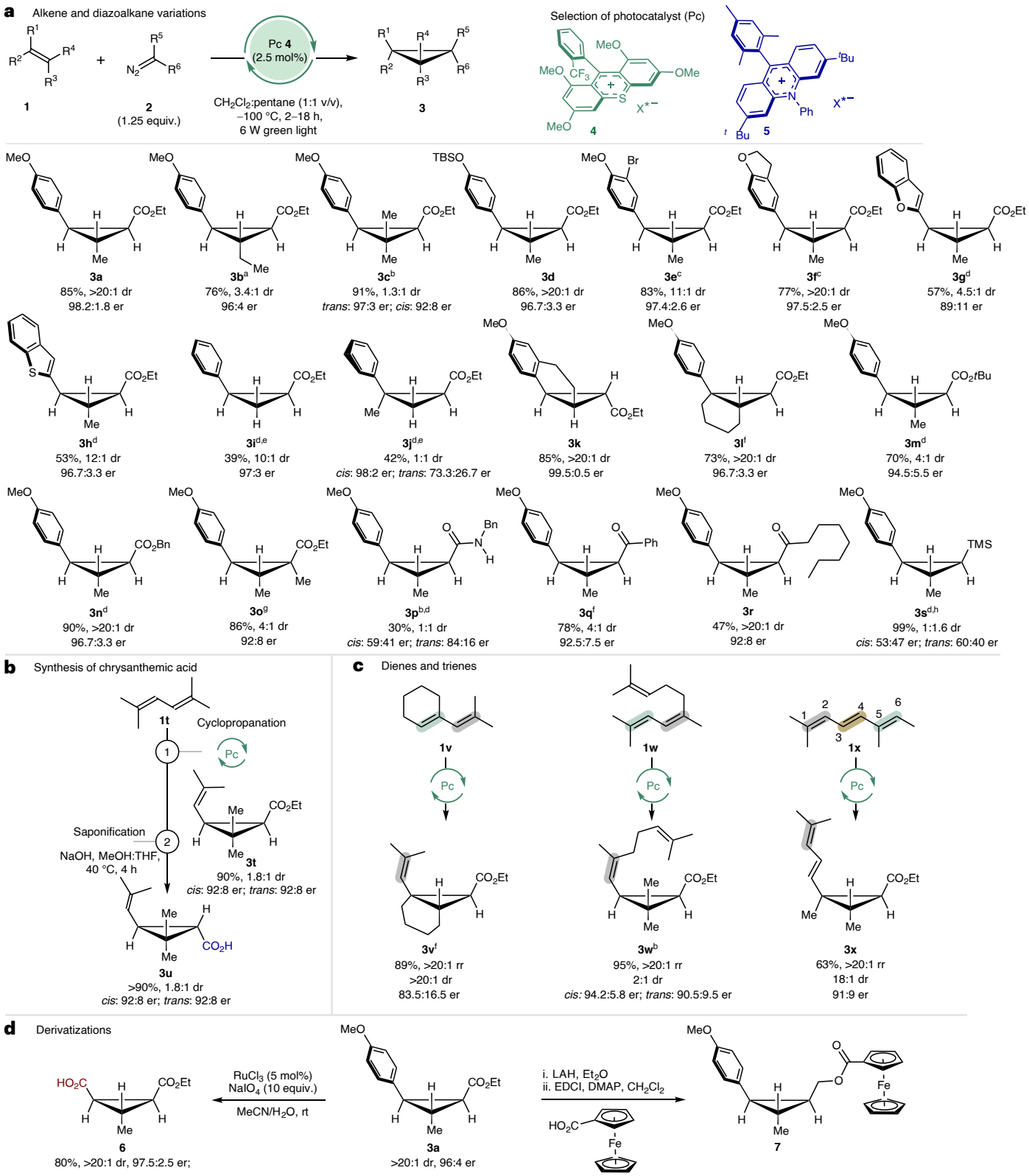

Fig. 3 | Substrate scope of the cyclopropanation methodology and derivatizations. a, Alkene and diazoalkane variations. **b**, Synthesis of chrysanthemic acid. **c**, Scope of the dienes and trienes. **d**, Derivatizations dr was determined by ^{1}HNMR. [a]Using catalyst **4E**. [b]Using catalyst **4C**. [c]Using 5 equiv. **2a** for 18 h. [d]Yield determined by ^{1}H NMR. [e]Using catalyst **5F** under 6 W of red light. [f]Using catalyst **4B**. [g]Using catalyst **4D**. [h]Using catalyst **5C** under 6 W of blue light. TBS, *tert*-butyldimethylsilyl; LAH, lithium aluminium hydride; EDCI, 1-ethyl-3-(3-dimethylaminopropyl)carbodiimid; DMAP, 4-dimethylaminopyridine.

https://doi.org/10.1038/s41929-025-01340-7

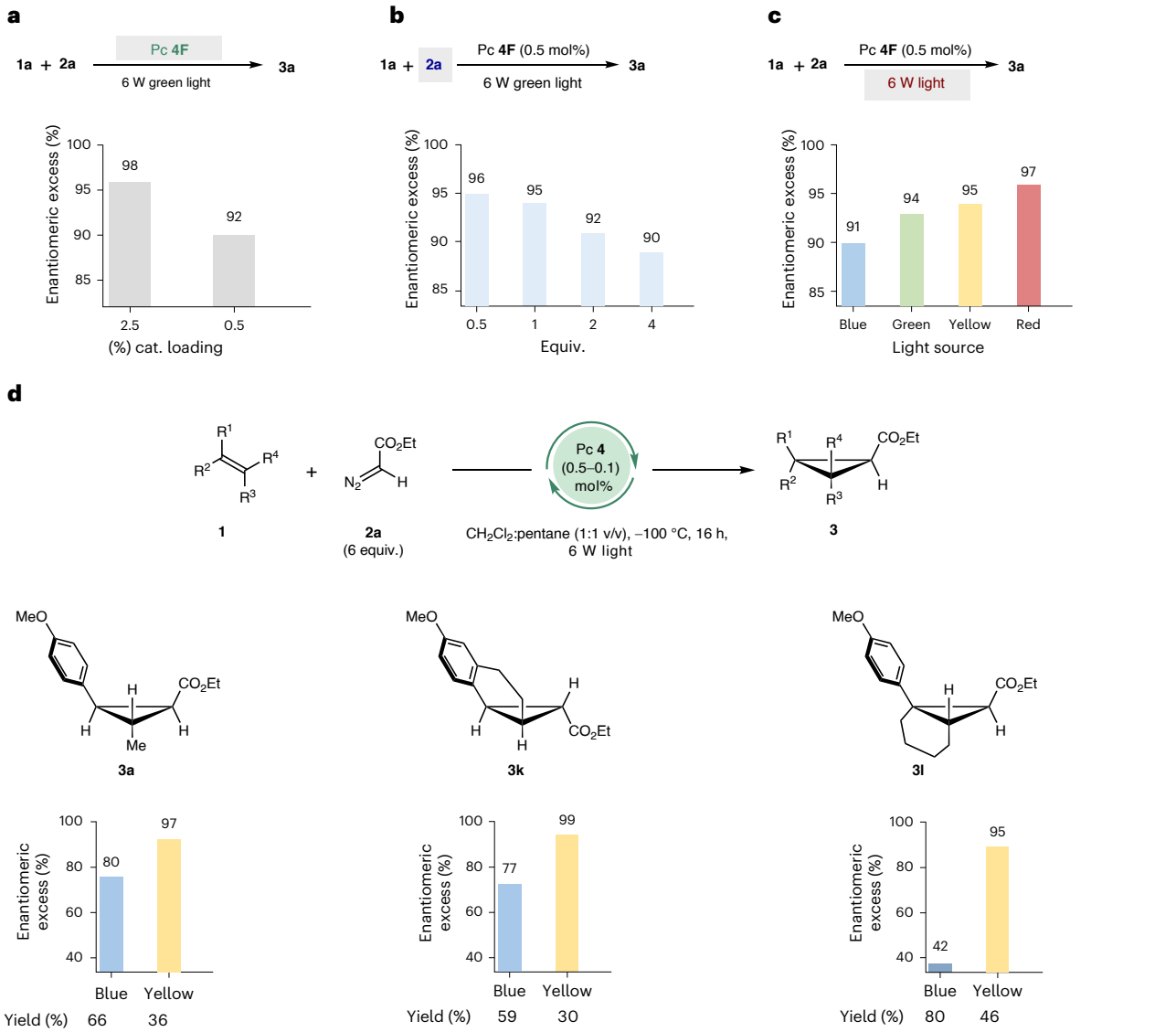

Fig. 4 | Reaction development for wavelength of light. a, Reaction development under lower catalyst loading conditions. **b**, Reaction development on the basis of the diazo compound **2a**. **c**, Reaction development under different light sources. **d**, Reactions with different olefins under blue and yellow light.

and also at a lower wavelength of 350 nm. Surprisingly, in addition to the usual emission spectra maximum at 627 nm, another maximum emission band was detected at 395 nm upon excitation at 350 nm (Fig. 5c). Interestingly the absorption band of the diazoester significantly superimposes with the emission band of the photocatalyst at lower wavelength (Fig. 5d), which led us to the hypothesis that it is this lower-wavelength excitation mode of the diazoester that is involved in the photochemical background pathway.

Steady-state fluorescence quenching experiments with the individual reactants were conducted to obtain Stern–Volmer plots and to identify the reagent that interacts with the excited state photocatalyst. Photocatalyst **4F** was first excited at 470 nm, and quenching experiments were performed separately with different amount of anethole **1a** and diazoester **2a**. The corresponding Stern–Volmer plots (Fig. 5e) clearly indicate that anethole **1a** is responsible for the fluorescence quenching, whereas diazoester **2a** has virtually no effect at this concentration. A separate set of steady-state florescence quenching experiments was conducted where the photocatalyst **4F** was excited at 350 nm. In contrast, the Stern–Volmer plot (Fig. 5f) shows significant fluorescence quenching with diazoester **2a**. Further standard radical probe and radical clock experiments were conducted to rule out radical process and support the radical cation mechanism, which is in line with the mechanism proposed in literature (Supplementary Fig. 3). To gain further information regarding the stereo-specificity of our reaction, we conducted control experiment with *Z*-anethole (Supplementary Fig. 4). Interestingly, under our optimized conditions, all four possible diastereoisomers were obtained in good yields. Under the optimized condition, control experiments were performed where interconversion of anethole was not observed (Supplementary Fig. 4). These experiments further strengthen the stepwise mechanism, which is also in line with the literature. Additionally, the redox potentials of our reactants, catalyst and product were measured (Supplementary Fig. 5).

Conclusions

Key to the success of our organocatalytic cyclopropanation of olefins with diazoalkanes has been the use of ACPC, exploiting the positive charge of the olefin radical cation intermediate towards ion pairing with an enantiopure counteranion. Our methodology is useful for a broad range of substrates and complements previously reported metal and metalloenzyme catalyzed cyclopropanations. It also addresses the

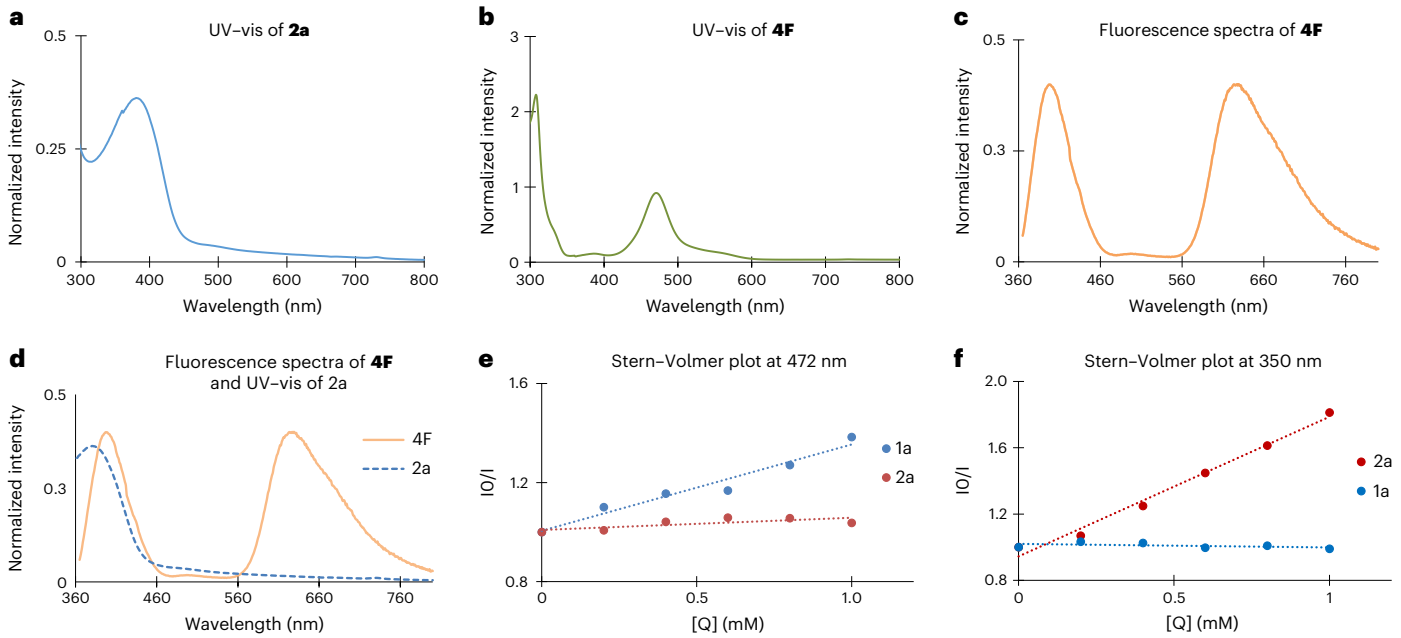

Fig. 5 | Spectroscopic analysis for mechanistic insights. a, The ultraviolet–visible (UV–vis) absorption spectra of **2a**. **b**, The UV–vis absorption spectra of **4F**. **c**, The emission spectra of **4F**. **d**, Overlay of the UV–vis spectrum of **2a** with the emission spectra of **4F**. **e**, A Stern–Volmer plot at excitation of 472 nm. **f**, A Stern–Volmer plot at excitation of 350 nm. Q, quencher's concentration.

unsolved problem of regioselectivity in the reaction of substrates with different olefins. The observed wavelength-dependent enantioselectivity could serve as a valuable mechanistic probe for photoredox catalysis, potentially aiding in distinguishing between alternative reaction pathways. Observing enantioselectivity in ACPC at one wavelength confirms the involvement of radical cations in the enantiodifferentiating step, whereas its absence at this or another wavelength is consistent with alternative mechanistic pathways, such as energy transfer that proceed via neutral intermediates. Our results underscore the potential of ACPC for controlling the selectivity of radical cations in alkene manipulations, complementing previous reports.

Methods

General procedure for anion exchange

The achiral anion of the photocatalysts was exchanged with the desired enantiopure anion using the salt metathesis technique. In a gas chromatography vial, photocatalyst (25–30 mg, 1.0 equiv.) and a corresponding chiral Brønsted acid catalyst (1.05 equiv.) were measured. Then, dichloromethane (300 µl) was added, followed by saturated $NaHCO_3$ solution (1.1 equiv., 400 µl). The reaction mixture was stirred vigorously for 30 min. Then, it was diluted with 1 ml of water and 1 ml of dichloromethane. The organic layer was separated, and the aqueous layer was extracted with dichloromethane (5 ml x3). The organic layer was collected and dried with Na_2SO_4, and the solvent was removed under reduced pressure. The obtained (>95% yield) solid colourful photocatalysts were used without further purification.

General procedure for the [2+1] cycloaddition reaction

A gas chromatography glass vial was charged with a magnetic stirring bar and photocatalyst (0.025 equiv., 2.5 mol%). The photocatalyst was dissolved in a 1:1 (v/v) solvent mixture of CH_2Cl_2 and pentane (0.1 M with respect to **1a**). At room temperature, anethole **1a** (1 equiv.) was added followed by diazoester **2a** (2 equiv.) in the dark. Then, the glass vial was transferred to a −100 °C cryostat and kept at this low temperature for 30 min and then irradiated with 6 W of green light. After the desired time, the light was switched off, and after 10 min, the reaction was then quenched with saturated K_2CO_3 in ethanol and allowed to warm up to room temperature. The crude reaction mixture was analysed by proton nuclear magnetic resonance (^{1}H NMR) using an internal standard and purified by SiO_2 flash column chromatography using 5–10% acetone in pentane as eluent.

Data availability

Details on the methods, optimization studies, mechanistic studies, spectroscopic data are available in the Supplementary Information. All other data and raw and unprocessed nuclear magnetic resonance data are available from the authors upon request. Crystallographic data for the structures reported in this Article have been deposited at the Cambridge Crystallographic Data Centre, under deposition no. CCDC 2429976 (7). Copies of the data can be obtained free of charge via CCDC at https://www.ccdc.cam.ac.uk/structures/.

References

1. Lin, H.-W. & Walsh, C. T. *The Chemistry of the Cyclopropyl Group* (Wiley, 1987).
2. Djerassi, C. & Doss, G. A. Structure and biosynthesis of cyclopropane-containing sterols of marine origin. *N. J. Chem.* **14**, 713–719 (1990).
3. Salaün, J. & Baird, M. S. Biologically active cyclopropanes and cyclopropenes. *Curr. Med. Chem.* **2**, 511–542 (1995).
4. Faust, R. Fascinating natural and artificial cyclopropane architectures. *Angew. Chem. Int. Ed.* **40**, 2251–2253 (2001).
5. Simmons, H. E. & Smith, R. D. A new synthesis of cyclopropanes from olefins. *J. Am. Chem. Soc.* **80**, 5323–5324 (1958).
6. Simmons, H. E. & Smith, R. D. A new synthesis of cyclopropanes. *J. Am. Chem. Soc.* **81**, 4256–4264 (1959).
7. Frühauf, H. W. Metal-assisted cycloaddition reactions in organotransition metal chemistry. *Chem. Rev.* **97**, 523–596 (1997).
8. Lebel, H., Marcoux, J.-F., Molinaro, C. & Charette, A. B. Stereoselective cyclopropanation reactions. *Chem. Rev.* **103**, 977–1050 (2003).
9. Krimse, W. Copper carbene complexes: advanced catalysts, new insights. *Angew. Chem. Int. Ed.* **42**, 1088–1093 (2003).

10. Merlic, C. A. & Zechman, A. L. Selectivity in rhodium(II) catalyzed reactions of diazo compounds: effects of catalyst electrophilicity, diazo substitution, and substrate substitution. From chemoselectivity to enantioselectivity. *Synthesis* **8**, 1137–1156 (2003).
11. Nishiyama, H. Cyclopropanation with ruthenium catalysts. *Top. Organomet. Chem.* **11**, 81–92 (2004).
12. Evans, D. A., Woerpel, K. A., Hinman, M. M. & Faul, M. M. Bis(oxazolines) as chiral ligands in metal-catalyzed asymmetric reactions. Catalytic, asymmetric cyclopropanation of olefins. *J. Am. Chem. Soc.* **113**, 726–728 (1991).
13. Doyle, M. P. & Protopopova, M. Highly enantioselective intramolecular cyclopropanation reactions of *N*-allylic-*N*-methyldiazoacetamides catalyzed by chiral dirhodium(II) carboxamidates. *Tetrahedron* **54**, 7919–7946 (1998).
14. Pellissier, H. Recent developments in asymmetric cyclopropanation. *Tetrahedron* **64**, 7041–7095 (2008).
15. Davies, H. M. L. & Manning, J. R. Catalytic C–H functionalization by metal carbenoid and nitrenoid insertion. *Nature* **451**, 417–424 (2008).
16. Liu, M., Le, N. & Uyeda, C. Nucleophilic carbenes derived from dichloromethane. *Angew. Chem. Int. Ed.* **62**, e202308913 (2023).
17. Coelho, P. S., Brustad, E. M., Kannan, A. & Arnold, F. Olefin cyclopropanation via carbene transfer catalyzed by engineered cytochrome P450 enzymes. *Science* **339**, 307–310 (2012).
18. Key, H. M., Dydio, P., Clark, D. S. & Hartwig, J. F. Abiological catalysis by artificial haem proteins containing noble metals in place of iron. *Nature* **534**, 534–537 (2016).
19. Huang, J. et al. Complete integration of carbene-transfer chemistry into biosynthesis. *Nature* **617**, 403–408 (2023).
20. Doyle, M. P., Dorow, R. L., Tamblyn, W. H. & Buhro, W. E. Regioselectivity in catalytic cyclopropanation reactions. *Tetrahedron Lett.* **23**, 2261–2264 (1982).
21. Aratani, T., Yoneyoshi, Y. & Nagase, T. Asymmetric synthesis of chrysanthemic acid. An application of copper carbenoid reaction. *Tetrahedron Lett.* **18**, 2599–2602 (1977).
22. Aratani, T., Yoneyoshi, Y. & Nagase, T. Asymmetric synthesis of chrysanthemic acid. An application of copper carbenoid reaction. *Tetrahedron Lett.* **16**, 1707–1710 (1975).
23. Itagaki, M. & Suenobu, K. Practical copper-catalyzed asymmetric synthesis of chiral chrysanthemic acid esters. *Org. Process Res. Dev.* **11**, 509–518 (2007).
24. Papageorgiou, C. D., Cubillo de Dios, M. A., Ley, S. V. & Gaunt, M. J. Enantioselective organocatalytic cyclopropanation via ammonium ylides. *Angew. Chem. Int. Ed.* **43**, 4641–4644 (2004).
25. Johansson, C. C. C. et al. Enantioselective catalytic intramolecular cyclopropanation using modified cinchona alkaloid organocatalysts. *Angew. Chem. Int. Ed. Engl.* **45**, 6024–6028 (2006).
26. Kunz, R. K. & MacMillan, D. W. C. Enantioselective organocatalytic cyclopropanations. The identification of a new class of iminium catalyst based upon directed electrostatic activation. *J. Am. Chem. Soc.* **127**, 3240–3241 (2005).
27. Sarabia, F. J. & Ferreira, E. M. Radical cation cyclopropanations via chromium photooxidative catalysis. *Org. Lett.* **19**, 2865–2868 (2017).
28. Cho, Y. H., Kim, J. H., An, H., Ahn, K.-H. & Kanga, E. J. Cycloaddition reactions of alkene radical cations using iron(III)-phenanthroline complex. *Adv. Synth. Catal.* **362**, 2183–2188 (2020).
29. Rybicka-Jasińska, K., Szeptuch, Z., Kubiszewski, H. & Kowaluk, A. Electrochemical cycloaddition reactions of alkene radical cations: a route toward cyclopropanes and cyclobutanes. *Org. Lett.* **25**, 1142–1146 (2023).
30. Das, S. et al. Asymmetric counteranion-directed photoredox catalysis. *Science* **379**, 494–499 (2023).
31. Yang, Z., Stivanin, M. L., Jurberg, I. D. & Koenigs, R. M. Visible light-promoted reactions with diazo compounds: a mild and practical strategy towards free carbene intermediates. *Chem. Soc. Rev.* **49**, 6833–6847 (2020).
32. Durka, J., Turkowska, J. & Gryko, D. Lightening diazo compounds? *ACS Sustain. Chem. Eng.* **9**, 8895–8918 (2021).
33. Langletz, T., Empel, C., Jana, S. & Koenigs, R. M. Stereoconvergent, photocatalytic cyclopropanation reactions of β-substituted styrenes with ethyl diazoacetate. *Tetrahedron Chem.* https://doi.org/10.1016/j.tchem.2022.100024 (2022).
34. Tanaka, K. et al. Redox potential controlled selective oxidation of styrenes for regio- and stereoselective crossed intermolecular [2 + 2] cycloaddition via organophotoredox catalysis. *Org. Lett.* **22**, 5207–5211 (2020).
35. Schreyer, L., Properzi, R. & List, B. IDPi Catalysis. *Angew. Chem. Int. Ed.* **58**, 12761–12777 (2019).

Acknowledgements

Generous support was received from the Max Planck Society, the Deutsche Forschungsgemeinschaft (German Research Foundation) under Germany's Excellence Strategy–EXC 2033–390677874–RESOLV and the European Research Council (Early stage organocatalysis) to B.L. We thank M. Meyer and H. Tüysüz for assistance with UV–vis and fluorescence spectroscopy. For help with cyclic voltammetry, we thank D. Spinnato and A. Stamoulis. The authors thank the technicians of our group and the members of our gas chromatography, mass spectrometry, HPLC, X-ray and NMR service departments.

Author contributions

B.L. and C.K.D. conceptualized the study. S.D., C.Z. and C.K.D. carried out the methodology. S.D., C.Z., A.G. and C.K.D. carried out the investigations. B.L. performed supervision. S.D. carried out writing of the original draft. S.D., C.Z., C.K.D. and B.L. carried out review and editing.

Funding

Open access funding provided by Max Planck Society.

Competing interests

B.L. is listed as an inventor on patent no. WO 2017/037141 filed by the Max-Planck-Institut für Kohlenforschung covering the IDPi catalyst class and its applications in asymmetric synthesis. Furthermore, B.L. and C.K.D. are listed as inventors on a patent on an improved synthesis of imidodiphosphoryl-derived catalysts using hexachlorophosphazonium salts (patent no. EP 3 981 775 A1) filed by the Max-Planck-Institut für Kohlenforschung. C.Z., S.D. and A.G. declare no competing interests.

Additional information

Supplementary information The online version contains supplementary material available at https://doi.org/10.1038/s41929-025-01340-7.

Correspondence and requests for materials should be addressed to Chandra Kanta De or Benjamin List.

Peer review information *Nature Catalysis* thanks the anonymous reviewers for their contribution to the peer review of this work.